Available online at www.sciencedirect.com
SCIENCE DIRECT
Bioorganic & Medicinal Chemistry
Bioorganic & Medicinal Chemistry 14 (2006) 3210–3217

Binding analysis of glycyrrhetinic acid to human serum albumin: Fluorescence spectroscopy, FTIR, and molecular modeling

Jianghong Tang, Feng Luan and Xingguo Chen*

Department of Chemistry, Lanzhou University, Lanzhou 730000, PR China

Received 16 November 2005; revised 18 December 2005; accepted 19 December 2005
Available online 18 January 2006

Abstract—Fluorescence spectroscopy, Fourier transform infrared spectroscopy (FTIR), and molecular modeling methods were employed to analyze the binding of glycyrrhetinic acid (GEA) to human serum albumin (HSA) under physiological conditions with GEA concentrations from 4.0×10^{-6} to 4.5×10^{-5} mol L^{-1}. The binding of GEA to HSA was via two types of sites: the numbers of binding site for the first type was near 0.45 and for the second type it was approximately 0.75. The binding constants of the second type binding site were lower than those of the first type binding site at corresponding temperatures, the results suggesting that the first type of binding site had high affinity and the second binding site involved other sites with lower binding affinity and selectivity. The fluorescence titration results indicated that GEA quenched the fluorescence intensity of HSA through static mechanism. The FTIR spectra evidence showed that the protein secondary structure changed with reduction of α-helices about 26.2% at the drug to protein molar ratio of 3. Thermodynamic analysis showed that hydrogen bonds were the mainly binding force in the first type of binding site, and hydrophobic interactions might play a main role in the second type of binding site. Furthermore, the study of computational modeling indicated that GEA could bind to the site I of HSA and hydrophobic interaction was the major acting force for the second type of binding site, which was in agreement with the thermodynamic analysis.

1. Introduction

Licorice (*Glycyrrhiza glabra*) has long history as a medicinal plant and is used throughout the world.[1,2] Glycyrrhizic acid (GIA), a triterpenoid saponin, is the main constituent of licorice root which is composed of one molecule of glycyrrhetinic acid (GEA) (structure shown in Fig. 1) and two molecules of glucuronic acid. GIA is hydrolyzed by glucuronidase of intestinal bacteria to its active principal aglycone, GEA, which is then absorbed into the blood.[3,4] The biological activities of GIA are associated with GEA, and include anti-inflammatory, anti-viral, anti-allergic, anti-hepatotoxic, and anti-tumor effects.[1,5] Recent studies indicate that GEA can delay the development of autoimmune disease[6] and decrease body fat mass.[7] As a potent inducer of mitochondrial permeability transition, it also can trigger the pro-apoptotic pathway.[8,2] Although the study of licorice's various pharmacological effects has been described well, there is no report of the binding of GEA to human serum albumin.

Knowledge of interaction mechanisms between drugs and plasma proteins is of crucial importance for us to understand the pharmacodynamics and pharmacokinetics of a drug. Drug binding influences the distribution, excretion, metabolism, and interaction with the target tissues. Drugs are mainly transported by human serum albumin (HSA), α_1-acidic glycoprotein (α_1-AGP), and

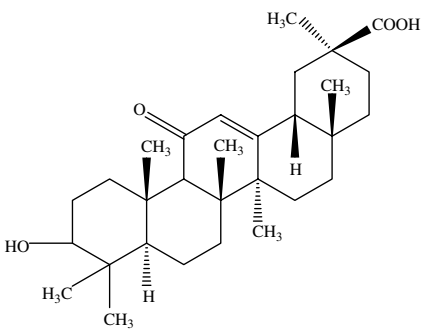

Figure 1. Chemical structure of glycyrrhetinic acid.

Keywords: Glycyrrhetinic acid; Human serum albumin; Fourier transform infrared spectroscopy; Fluorescence spectroscopy; Molecular modeling.
* Corresponding author. Tel.: +86 931 8912540; fax: +86 931 8912582; e-mail: chenxg@lzu.edu.cn

0968-0896/$ - see front matter © 2005 Elsevier Ltd. All rights reserved.
doi:10.1016/j.bmc.2005.12.034

lipoproteins in blood. HSA is the most abundant plasma protein, which accounts for approximately 60% of the total protein corresponding to a concentration of 40 mg ml^{-1} (~0.6 mM) in the blood.[9] It has many important physiological and pharmacological functions[10], and has been one of the most extensively studied of all proteins. The main function of it is to regulate plasma osmotic pressure between the blood and tissues, and is chiefly responsible for the maintenance of blood pH. The other most important property of it is that it serves as a depot protein and as a transport protein for a variety of endogenous and exogenous compounds such as fatty acids, hormones, bilirubin, drugs, and a large diverse of metabolites.[11–13] Investigating the interaction of drugs to HSA can elucidate the properties of drug–protein complex, as it may provide useful information of the structural features that determine the therapeutic effectiveness of drugs. Therefore, it has become an important research field in life sciences, chemistry, and clinical medicine.[14,15] There are some works to study the interaction of drug with protein by fluorescence technique, Fourier transform infrared spectroscopy (FTIR), circular dichroism (CD) spectroscopy, and molecular modeling.[16–24] However, none of the investigations determine in detail the GEA–HSA binding mode, binding constant, and the effects of GEA on the protein secondary structure.

Fluorescence and FTIR are powerful tools to study the interaction between small molecule ligand and bio-macromolecule. The aim of this work was to analyze the binding properties (including binding mechanism, binding constant, and the number of binding sites) of GEA to HSA and thermodynamic function for this reaction at four different temperatures (291, 301, 310, and 318 K) under physiological pH conditions. Another purpose of this work was to check the effect of GEA on HSA secondary structure changes using FTIR. Furthermore, the molecular modeling was also used to interpret the binding location of GEA on HSA.

2. Results and discussion

2.1. Analysis of fluorescence quenching of HSA by GEA

The fluorescence of HSA comes from the tryptophan, tyrosine, and phenylalanine residues. Actually, the intrinsic fluorescence of HSA is almost contributed by tryptophan alone, because phenylalanine has a very low quantum yield and the fluorescence of tyrosine is almost totally quenched if it is ionized or near an amino group, a carboxyl group, or a tryptophan. This viewpoint was well supported by the experimental observation of Sulkowska.[25] That is, the change of intrinsic fluorescence intensity of HSA is that of tryptophan residue when small molecule substances bound to HSA. Figure 2 shows the fluorescence emission spectra of HSA in the absence and presence of GEA. It can be seen that HSA had a strong fluorescence emission band at 336 nm, while GEA had no intrinsic fluorescence at the excitation wavelength of 280 nm. And the fluorescence emission intensity of HSA decreased regularly

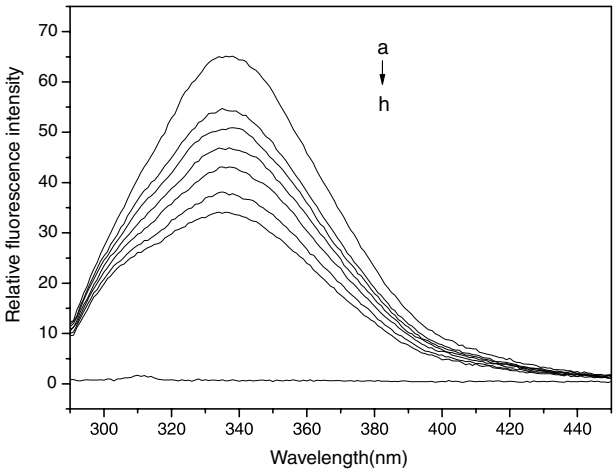

Figure 2. Fluorescence emission spectra excited at 280 nm (pH 7.40, $T = 291$ K) (a) 3.0×10^{-6} mol L^{-1} HSA; (b–g) 3.0×10^{-6} mol L^{-1} HSA in the presence of 0.30, 0.50, 1.0, 1.8, 3.1, and 4.5×10^{-5} mol L^{-1} GEA, respectively; (h) 1.67×10^{-5} mol L^{-1}GEA.

with the increase of concentration of GEA. The strong quenching of the HSA fluorescence indicated that the microenvironment around the Trp 214 residue was changed after the addition of GEA.[26]

Quenching can be induced by different mechanisms, which were usually classified into dynamic quenching and static quenching. Dynamic and static quenching can be distinguished by their difference depending on temperature. Higher temperature results in faster diffusion and larger amounts of collisional quenching and will typically lead to the dissociation of weakly bound complexes and smaller amounts of static quenching. Therefore, the quenching constant increases with increasing temperature for dynamic quenching, however, it decreases with increasing temperature for static quenching.

Here, quenching data from the fluorescence titration experiments can be analyzed according to the modified Stern–Volmer equation.[27]

$$\frac{F_0}{F_0 - F} = \frac{1}{fK[\mathrm{Q}]} + \frac{1}{f}, \tag{1}$$

where F_0 and F are the relative fluorescence intensities of protein in the absence and presence of quencher, respectively; K is the Stern–Volmer quenching constant and [Q] is the quencher concentration; f is the fractional maximum fluorescence intensity of the protein summed up. The plot of $F_0/(F_0 - F)$ versus 1/[Q] is linear with (1/fK) as the slope and 1/f as the intercept. Quenching constant K is a quotient of intercept 1/f and slope (1/fK).

Figure 3 shows the Stern–Volmer plots for the GEA–HSA system at four different temperatures (291, 301, 310, and 318 K). In the range of GEA concentrations from 4.0×10^{-6} to 4.5×10^{-5} mol L^{-1} (concentration of HSA was 3.0×10^{-6} mol L^{-1}), the Stern–Volmer plots had two regression curves intersecting at $C_{\mathrm{GEA}}/C_{\mathrm{HSA}} \approx 5.2$. The curvature with increase of the GEA

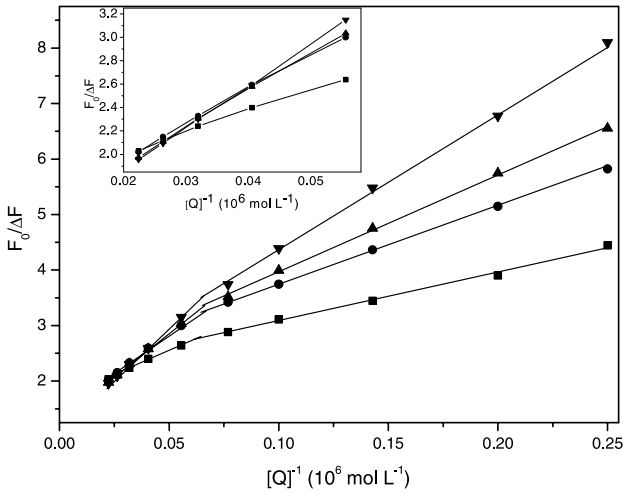

Figure 3. The modified Stern–Volmer plots of the HSA-eupatilin at different temperatures (■, 291 K; ●, 301 K; ▲, 310 K; ▼, 318 K). $C_{HSA} = 3.0 \times 10^{-6}$ mol L^{-1}, $C_{GEA} = 4.0 \times 10^{-6}$ to 4.5×10^{-5} mol L^{-1}. pH 7.40, $\lambda_{ex} = 280$ nm, $\lambda_{em} = 337$ nm.

concentration suggested the existence of additional binding sites for high GEA concentration.[27,28] The constant K calculated from the Stern–Volmer equation is listed in Table 1. It can be seen from the Table, the quenching constant (K_1 and K_2) decreased with increasing temperature, which coincides with the static type of quenching mechanism. As static quenching, the quenching constant can be interpreted as the association constant of the complexation reaction since static quenching arises from the formation of a ground state complex that is nonfluorescent or weakly fluorescent between fluorophore and quencher.[29]

The synchronous fluorescence spectra present the information about the molecular microenvironment in the vicinity of the fluorophore functional groups. In the synchronous fluorescence of HSA, the shift in position of maximum emission wavelength corresponds to the changes of polarity around the fluorophore of amino acid residues. The $\Delta\lambda$ values (scanning interval, $\Delta\lambda = \lambda_{emission} - \lambda_{excitation}$) stabilized at 15 or 60 nm, synchronous fluorescence of HSA gives the characteristic information of tyrosine residues and tryptophan residues, respectively.[30] The effect of GEA on HSA synchronous fluorescence spectroscopy is shown in Figure 4. As can be seen from the figure, the fluorescence of tyrosine residues was weak and the position of maximum emission wavelength had no change when $\Delta\lambda$ was 15 nm. And the fluorescence of tryptophan residues

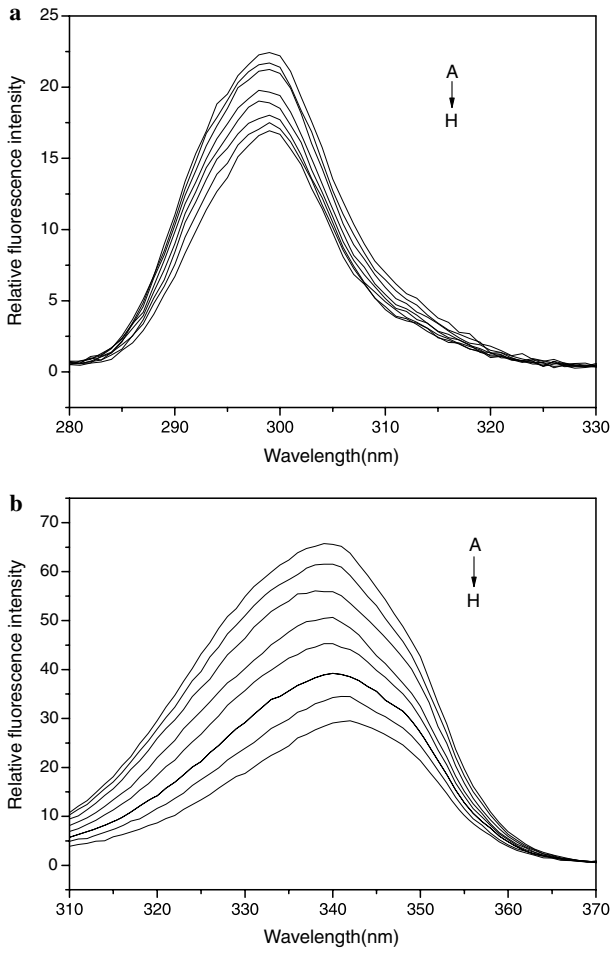

Figure 4. Synchronous fluorescence spectrum of HSA in the absence and presence of GEA (pH 7.40, $T = 291$ K): (a) $\Delta\lambda = 15$; (b) $\Delta\lambda = 60$. (A) 3.0×10^{-6} mol L^{-1} HSA; (B–H) 3.0×10^{-6} mol L^{-1} HSA in the presence of 0.10, 0.23, 0.57, 1.3, 2.4, 3.8, and 5.4×10^{-5} mol L^{-1} GEA, respectively.

was strong and the maximum emission wavelength moderately shifted toward long wave when $\Delta\lambda$ was 60 nm. This reflects the fact that the microenvironment of the tryptophan residue was significantly affected by GEA binding. It is reported that the maximum emission wavelength (λ_{max}) at 330–332 nm indicates that tryptophan resides are located in the nonpolar region, namely, they are buried in a hydrophobic cavity in HSA; λ_{max} at 350–352 nm shows that tryptophan residues are exposed to water, namely, the hydrophobic cavity in HSA is disagglomerated and the structure of HSA is looser. The red-shift effect suggests that GEA bound to the hydrophobic cavity of HSA results in the loose structure of HSA and

Table 1. Binding parameters for the interaction of the GEA and HSA at pH 7.40 measured by fluorimetric titration

Temperatures (K)	Modified Stern–Volmer		Scatchard method			
	$C_{GEA}/C_{HSA} < 5.2$	$C_{GEA}/C_{HSA} > 5.2$	$C_{GEA}/C_{HSA} < 5.2$		$C_{GEA}/C_{HSA} > 5.2$	
	K_1 ($\times 10^5$ L mol^{-1})	K_2 ($\times 10^4$ L mol^{-1})	K_1 ($\times 10^5$ L mol^{-1})	n_1	K_2 ($\times 10^4$ L mol^{-1})	n_2
291	2.77	7.35	2.74	0.44	7.32	0.61
301	1.66	4.68	1.65	0.43	4.58	0.73
310	1.21	3.99	1.18	0.46	3.92	0.79
318	0.776	3.21	0.743	0.54	3.23	0.86

the polarity around the tryptophan residues was increased and the hydrophobicity was decreased.[31]

2.2. Changes of the HSA secondary structure induced by GEA binding

To test the changes of the HSA secondary structure after GEA bound to HSA, the FTIR spectroscopy was investigated. Infrared spectra of proteins exhibit a number of amide bands, which represent different vibrations of peptide moieties. Among the amide bands of the protein, amide I band ranging from 1600 to 1700 cm^{-1} (mainly C=O stretch) and amide II band 1548 cm^{-1} (C–N stretch coupled with N–H bending mode) have been widely used as the typical ones.[32,33] They both have relationship with the secondary structure of the protein. However, the amide I band is more sensitive to the change of protein secondary structure than amide II.[33] The FTIR spectra and difference spectra of HSA are shown in Figure 5. From Figures 5a and b, it can be seen that the peak positions of amide I bands shifted from 1656.40 to 1637.83 cm^{-1} in HSA infrared spectrum after interaction with GEA. The changes of these peak positions and peak shapes demonstrated that the secondary structures of the HSA were changed by the interaction of GEA with HSA.

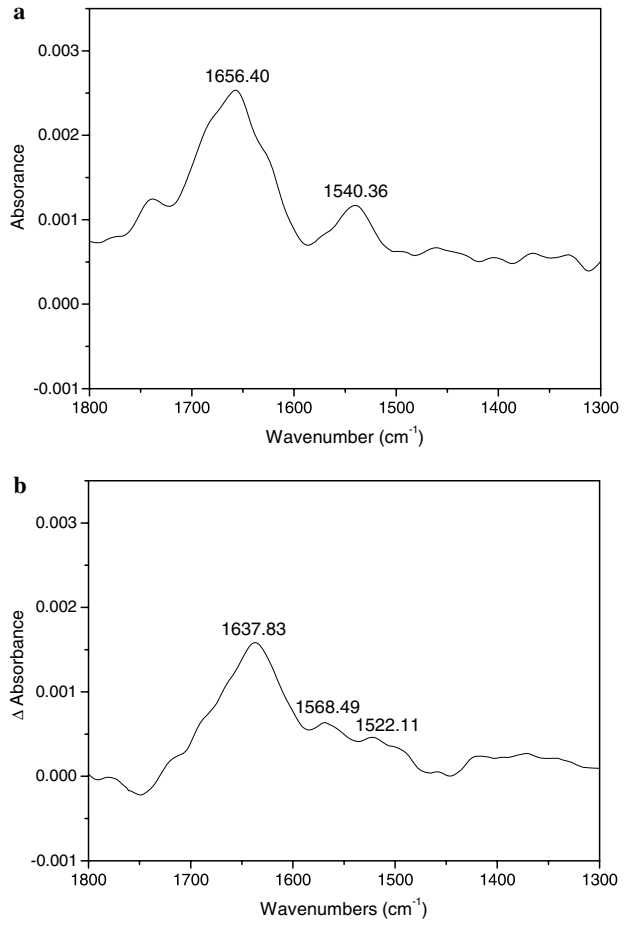

Figure 5. FTIR spectra and difference spectra of HSA. (a) The FTIR spectra of free HSA (subtracting the absorption of the buffer solution from the spectrum of the protein solution); (b) the FTIR difference spectra of HSA (subtracting the absorption of the GEA-free form from that of GEA–HSA bound form), in buffer solution of pH 7.40, $C_{HSA} = 3.0 \times 10^{-6}$ mol L^{-1}, $C_{GEA} = 9.0 \times 10^{-6}$ mol L^{-1}.

A quantitative analysis of the protein secondary structure for the free HSA and GEA–HSA complex in aqueous is given in Figure 6. According to the literature,[34] before estimation of the percentage content of each secondary structure, the component bands should be assigned. The band range 1610–1640 cm^{-1} is generally assigned to β-sheet, 1640–1650 cm^{-1} to random coil, 1650–1658 cm^{-1} to α-helix, and 1660–1700 cm^{-1} to β-turn structure. The percentages of each secondary structure of HSA can be calculated based on the integrated areas of the component bands in amide I. The free HSA contained α-helical (50.93%), β-sheet (25.46%), and β-turn structures (23.61%). With regard to the GEA–HSA complex, the α-helical structure reduced from 50.93% to 24.73%, β-turn increased from 23.61%

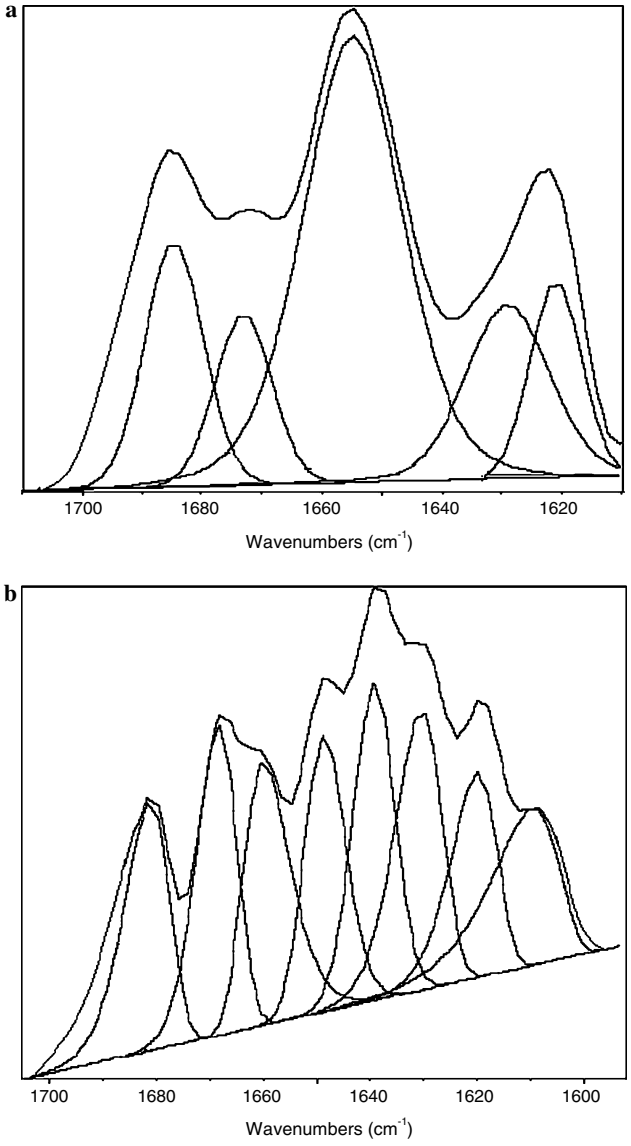

Figure 6. The curve-fit amide I (1700–1600 cm^{-1}) region and secondary structure determination of the free HSA (a) and GEA–HSA complexes (b) in buffer solution of pH 7.40. $C_{HSA} = 3.0 \times 10^{-6}$ mol L^{-1}, $C_{GEA} = 9.0 \times 10^{-6}$ mol L^{-1}.

to 25.27%, and a random coil appeared (13.98%) after interaction of GEA with HSA.

2.3. Analysis of binding reaction

Some studies have suggested that HSA was able to bind many ligands in several binding sites. Site I of HSA showed affinity for warfarin,[35] bilirubin,[36] etc., and site II for diazepam[37] and ibuprofen,[35] etc. Both the 1-anilinonaphthalene-8-sulfonate with bovine serum albumin[38] and anti-coagulant rodenticides diphacinone with human serum albumin[39] could bind either on the high affinity binding site or on the low affinity binding site. Indeed, binding to albumin is often of high specificity for low concentrations of the ligand, but for high ratio ligand–albumin, additional ligand molecules can associate with low affinity.[11,40]

In drug–protein binding studies, fluorescence quenching data were also used to calculate the binding constants and the number of binding sites by Scatchard equation.[41]

$$r/D_f = nK - rK. \quad (2)$$

In Eq. 2, r represents the number of moles of bound drug per mole of protein, D_f represents the concentration of unbound drug, K is the binding constant, and n is the number of binding sites. The plot of r/D_f versus r gives the binding constant. The results are presented in Figure 7 and Table 1. In Figure 7, the Scatchard plots for the GEA–HSA at four different temperatures had no single linear relationship but had two regression curves intersecting at $C_{GEA}/C_{HSA} \approx 5.2$, which suggested there were two types of binding sites in the interaction of GEA with HSA. The report [42] showed when the molecular ratios of ligand HB to HSA become larger than 1:1, some of HB molecules may be multiple-bound to a certain site of HSA. It can be seen from Table 1, the binding constants (K_1 and K_2) obtained from modified Stern–Volmer equation were in good agreement with that obtained from Scatchard equation. And the number of binding sites (n_1 and n_2) was lower than 1, which implied that the GEA was only partially bound to HSA. When C_{GEA}/C_{HSA} was lower than 5.2, the value of n_1 for the first type was near 0.45 and the K_1 value of this type of site peaked at 291 K and then decreased to a minimum at 310 K. When C_{GEA}/C_{HSA} was higher than 5.2, the value of n_2 for the second type was approximately 0.75 and the corresponding K_2 value also decreased gradually by increasing the temperature. Moreover, the binding constants K_2 were lower than K_1 at corresponding temperatures. The results indicated that at low concentration, the first type of binding site had high affinity, while at high concentration GEA involved other sites with lower binding affinity and selectivity, accordingly resulting in the decrease in binding constants. [27,40] In this article, the binding constants obtained from the Scatchard equation were applied to analyze the thermodynamic parameter and nature of the binding forces.

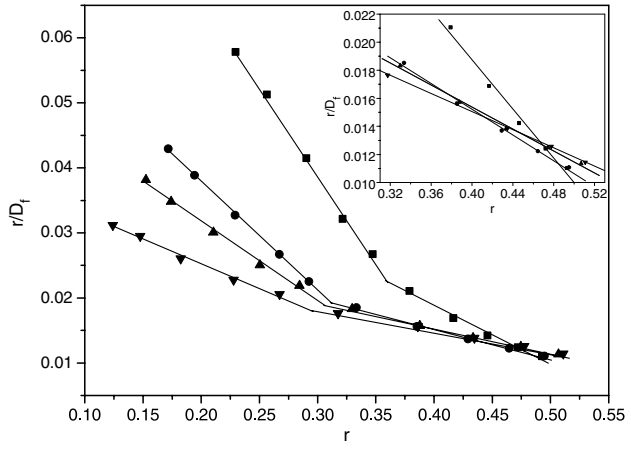

Figure 7. The Scatchard plots of the HAS–eupatilin at different temperatures (■, 291 K; ●, 301 K; ▲, 310 K; ▼, 318 K). $C_{HSA} = 3.0 \times 10^{-6}$ mol L^{-1}, $C_{GEA} = 4.0 \times 10^{-6}$ to 4.5×10^{-5} mol L^{-1}. pH 7.40, $\lambda_{ex} = 280$ nm, $\lambda_{em} = 337$ nm.

2.4. Thermodynamic analysis and the nature of the binding forces

The binding forces between small molecule and biomacromolecule may include hydrophobic force, electrostatic interactions, van der Waals interactions, hydrogen bonds, etc. The thermodynamic parameters of binding reaction are the main evidence for confirming the binding force. For this purpose, the temperature-dependence of the binding constant was measured at four different temperatures (291, 301, 310, and 318 K). If the enthalpy change (ΔH^0) does not vary significantly over the temperature range studied, then its value and that of entropy change (ΔS^0) can be determined from the van't Hoff Eq. 3. The free energy change (ΔG^0) of the binding reaction at different temperature was calculated from Eq. 4.

$$\ln K = -\Delta H^0/RT + \Delta S^0/R \quad (3)$$

$$\Delta G^0 = \Delta H^0 - T \cdot \Delta S^0, \quad (4)$$

where K is the binding constant at the corresponding temperature T, R is the gas constant, and T is absolute

Table 2. Thermodynamic parameters of the two types of binding sites for the binding of GEA to HSA at pH 7.40

Temperature (K)	ΔH^0 (kJ mol^{-1})		ΔS^0 (J mol^{-1} K^{-1})		ΔG^0 (kJ mol^{-1})	
	n_1	n_2	n_1	n_2	n_1	n_2
291	−36.33	−22.70	−20.66	14.72	−30.32	−26.98
301	−36.33	−22.70	−20.66	14.72	−30.11	−27.13
310	−36.33	−22.70	−20.66	14.72	−29.93	−27.26
318	−36.33	−22.70	−20.66	14.72	−29.76	−27.37

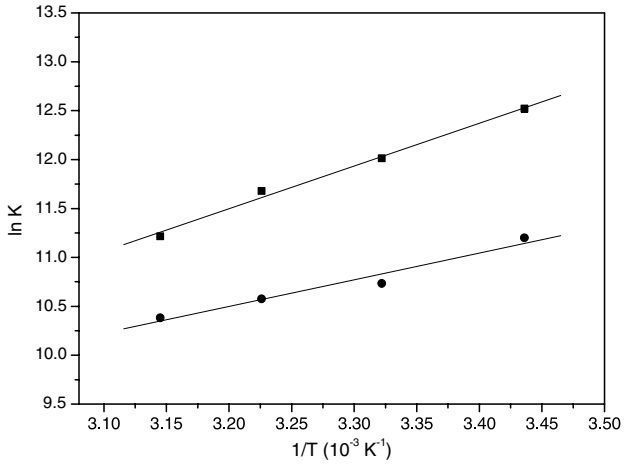

Figure 8. Variation of ln$K$ as a function of $1/T$ for the two types of binding sites. (■), K_1; (●), K_2.

temperature. There was good linear relationship between ln K and $1/T$ (Fig. 7) for each type of binding site, which showed that the assumption of near constant ΔH^0 was justified. The values of ΔH^0, ΔS^0, and ΔG^0 are listed in Table 2. For the two types of binding sites, the negative ΔG^0 and negative ΔH^0 meant that the binding process was spontaneous and the formation of the GEA–HSA complex was an exothermic reaction. The interaction of the first kind had a ΔS^0 value of -20.66 J mol^{-1} K^{-1}, which denoted the formation of a much more orderly system than that made up of the ligand and protein in isolation. The sign and magnitude of the thermodynamic parameters associated with various individual kinds of interaction that may take place in protein association processes were characterized.[43] From the viewpoint of water structure, the first type of binding site had negative ΔH^0 (-36.33 kJ mol^{-1}) and negative ΔS^0 (-20.66 J mol^{-1} K^{-1}), both of which were typical of hydrogen bonds. Positive ΔS^0 (14.72 J mol^{-1} K^{-1}) of the second type of binding site was considered as the evidence for hydrophobic interactions. In addition, a specific electrostatic interaction between ionic species in an aqueous solution is characterized by a positive ΔS^0 value and negative ΔH^0 value. In the present work, GEA was a kind of acid. Under experiment conditions (pH 7.40) it might be partially ionized. The contribution of the ΔH^0 term to ΔG^0 (301 K) was about 81.6% for the interaction of GEA and HSA via the second type of binding site. Therefore, we inferred that hydrophobic interaction might play a major role in the interaction of GEA with HSA, electrostatic interactions appearing to play some role in the second type binding site (Fig. 8).

2.5. Computational modeling of the GEA–HSA complex

The investigation of 3-D structure of crystalline albumin showed that HSA contains three homologous domains (I, II, and III): I (residues 1–195), II (196–383), and III (384–585). And each domain can be divided into two subdomains (A and B).[44] The crystallographic analysis[10,45] has revealed that HSA has binding sites of compounds within hydrophobic cavities in subdomains IIA and IIIA, which are corresponding to site I and site II, respectively, and sole tryptophan residue (Trp 214) of HSA is in subdomain IIA. There is a large hydrophobic cavity present in subdomain IIA that many drugs can bind to.

The crystal structure of HSA in complex with warfarin was taken from the Brookhaven Protein Data Bank (entry codes 1 h9z). The potential of the 3-D structure of HSA was assigned according to the Amber 4.0 force field with Kollman-all-atom charges. The initial structure of the GEA was generated by molecular modeling software Sybyl 6.9. The geometry of the molecule was subsequently optimized to minimal energy using the Tripos force field with Gasteiger–Marsili charges. Then it was used to replace warfarin in the HSA-warfarin crys-

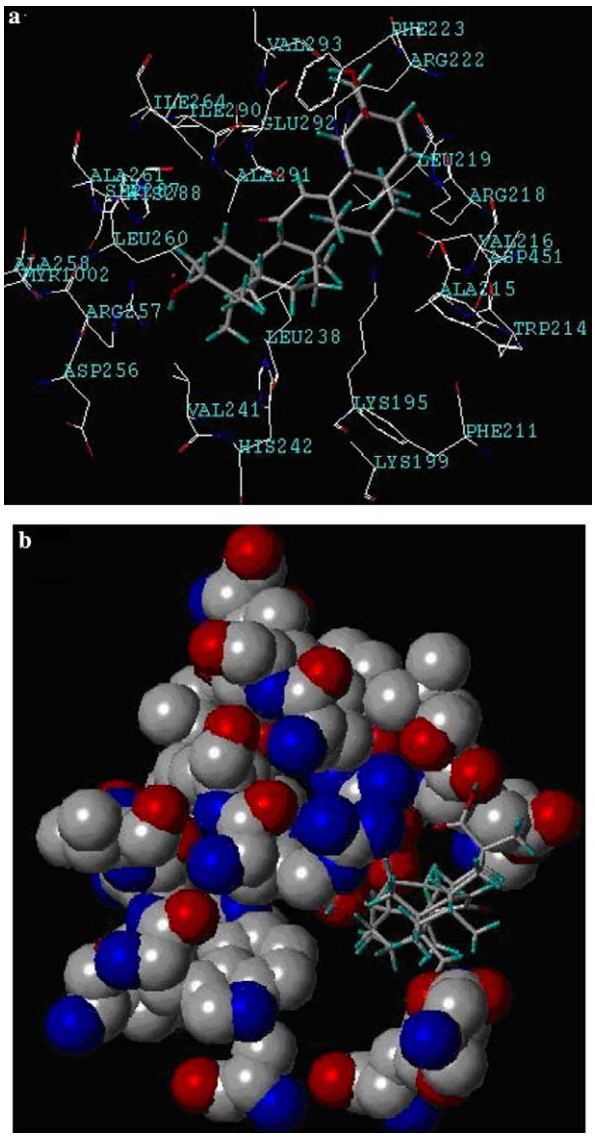

Figure 9. The interaction model between GEA and HSA. (a) Only residues around 6.5 Å of GEA are displayed. The residues of HSA are represented using lines and the GEA structure is represented using a stick model. (b) GEA–HSA spacefill conformation. Protein atoms are shown in CPK representation and the GEA structure is represented using a stick model.

tal structure. At last, FlexX program was used to establish the interaction modes between the GEA and HSA. The computational modeling study was applicable to the second type of binding site in the analysis of binding reaction. It was the reason that the molar ratio of GEA to HSA of the second type of binding site was nearly 1:1. Figures 9a and b exhibit the optimal energy ranked result of GEA interaction with the residues of HSA and the GEA–HSA spacefill conformation. It can be seen that the GEA molecule was situated within subdomain IIA hydrophobic cavity. GEA molecule moiety was located within the binding pocket and several methyl groups of GEA were adjacent to hydrophobic residues Leu (219), Leu (238), Val (241), Val (216), Trp (214), etc., of subdomain IIA of HSA (site I). This fact suggested that there were hydrophobic interactions between GEA and HSA. Furthermore, this phenomenon provided a good structural basis to explain the very efficient fluorescence quenching of HSA emission in the presence of GEA. The results of molecular modeling suggested that the interaction between HSA and GEA was dominated by hydrophobic force, which was in agreement with the binding mode proposed in thermodynamic analysis and nature of the binding forces.

3. Conclusions

The binding of GEA to HSA was analyzed by means of fluorescence spectroscopy, FTIR, and molecular modeling. The fluorescence titration results showed that this binding was via two types of binding sites: one with a high affinity but relatively fewer binding number and the other with a lower binding constant but greater binding number. The number of binding sites of each type of site and their respective binding constants were calculated at the four temperatures (291, 301, 310, and 318 K). The binding constants of the second type binding site were lower than those of the first type binding site at corresponding temperatures, the results suggesting that the first type of binding site had high affinity and the second binding site involved other sites with lower binding affinity and selectivity. FTIR spectra evidence showed that the secondary structure of HSA was changed after GEA bound to it. By thermodynamic analyzing, it can be concluded that hydrogen bonds were the leading binding force in the first type of binding site, and hydrophobic interactions might play a main role in the second type of binding site. Furthermore, the results of computational modeling indicated that GEA could bind to the site I of HSA and hydrophobic interaction was the major acting force, which was in agreement with the thermodynamic analysis.

4. Materials and methods

4.1. Materials and preparation of solutions

Glycyrrhetinic acid (GEA, analytical grade) was purchased from The National Institute for the Control of Pharmaceutical and Biological Products (China). HSA (fatty acid free <0.05%) was purchased from Sigma Chemical Company, it was used without further purification, and its molecular weight was assumed to be 66,500 to calculate the molar concentrations. NaCl (analytical grade, 0.5 mol L^{-1}) solution was used to keep the ion strength at 0.1. Tris–HCl (0.05 mol L^{-1}) buffer solution containing 0.1 mol L^{-1} NaCl was used to keep the pH of the solution at 7.40. HSA stock solution of 3.0×10^{-5} mol L^{-1} was prepared with the Tris–HCl buffer solution and kept in the dark at 4 °C. The stock solution (1.0×10^{-3} mol L^{-1}) of GEA was prepared in anhydrous methanol. All other reagents were of analytical grade and double-distilled water was used throughout the experiments.

4.2. Apparatus and methods

A RF-5301PC Spectrofluorimeter (Shimadzu, Japan) was used to record the fluorescence spectra and intensities, both excitation and emission bandwidths set on 5 nm. An electronic thermoregulating water bath (NTT-2100, EYELA, Japan) was used to control the temperature of the samples.

Fluorescence emission spectra were read in the range of wavelength from 290 to 450 nm using an excitation wavelength of 280 nm. Fluorometric titration experiments: 3.0 ml solution containing appropriate concentration of HSA was titrated in the Tris buffer solution (pH 7.40) by successive additions of GEA stock solution (the final range of GEA concentrations was from 4.0×10^{-6} to 4.5×10^{-5} mol L^{-1}). Titrations were done manually by using trace syringes, and the fluorescence intensities were recorded at excitation and emission wavelengths of 280 and 337 nm. The GEA was added from a concentrated stock solution so that volume increment was negligible. All experiments were performed at four temperatures (291, 301, 310, and 318 K). The temperature of sample was kept by recycling water throughout the experiment. Synchronous fluorescence spectra of HSA (3.0×10^{-6} mol L^{-1}) in the presence of GEA (1.0×10^{-6} to 5.4×10^{-5} mol L^{-1}) were recorded. The wavelength ranges of synchronous scanning were from 310 to 370 nm ($\Delta\lambda = 60$ nm) and 280 to 330 nm ($\Delta\lambda = 15$ nm) at room temperature.

All infrared spectra were recorded at room temperature with a Nicolet Nexus 670 FTIR Spectrometer (America) equipped with a germanium attenuated total reflection (ATR) accessory, a deuterated triglycine sulfate (DTGS) detector, and a KBr beam splitter. All spectra were taken via the ATR method with a resolution of 4 cm^{-1} and 60 scans. The infrared spectra of HSA and the GEA–HSA complex (the molar ratio of GEA to HSA was 3:1) were obtained in the featured region of 1800–1300 cm^{-1}. The FTIR spectrum of free HSA was acquired by subtracting the absorption of the Tris buffer solution from the spectrum of the protein solution, and the difference spectrum of HSA was obtained by subtracting the spectrum of GEA-free form from that of GEA–HSA form with the same concentration. The subtraction criterion was that the original spectrum of the protein solution between 2200 and 1800 cm^{-1} was featureless.[46] Fourier self-deconvolution and secondary

derivative were applied to the range of 1600–1700 cm^{-1} to estimate the number, position, and width of component bands. Based on these parameters, curve-fitting process was carried out by Galactic Peaksolve software (version 1.0) to get the optimal Gaussian-shaped curves that fit the original protein spectrum. After the identification of the individual bands, the content of each representative structure of HSA was calculated using the area of their respective component bands.

Acknowledgment

The project was supported by the National Natural Science Foundation of China (No. 20275014).

References and notes

1. Armanini, D.; Fiore, C.; Mattarello, M. J.; Bielenberg, J.; Palermo, M. *Exp. Clin. Endocr. Diab.* **2002**, *110*, 257.
2. Fiore, C.; Salvi, M.; Palermo, M.; Sinigaglia, G.; Armanini, D.; Toninello, A. *Biochim. Biophys. Acta* **2004**, *1658*, 195.
3. Takeda, S.; Ishthara, K.; Wakui, Y.; Amagaya, S.; Maruno, M.; Akao, T.; Kobashi, K. J. *Pharm. Pharmacol.* **1996**, *48*, 902.
4. Akao, T. *Biol. Pharm. Bull.* **1998**, *21*, 1036.
5. Shibata, S. *Planta. Med.* **2000**, *120*, 849.
6. Horigome, H.; Hirano, T.; Oka, K. *Life Sci.* **2001**, *69*, 2429.
7. Armanini, D.; De Palo, C. B.; Mattarello, M. J.; Spinella, P.; Zaccaria, M.; Ermolao, A.; Palermo, M.; Fiore, C.; Sartorato, P.; Francini-Pesenti, F.; Karbowiak, I. *Endocrinol. J. Invest.* **2003**, *26*, 646.
8. Salvi, M.; Fiore, C.; Armanini, D.; Toninello, A. *Biochem. Pharmacol.* **2003**, *66*, 2375.
9. Peters, T. *All About Albumin: Biochemistry, Genetics and Medical Applications*; Academic Press: San Diego, CA, 1996.
10. He, X. M.; Carter, D. C. *Nature* **1992**, *358*, 209.
11. Kragh-Hansen, U. *Pharmacol. Rev.* **1981**, *33*, 17.
12. Benet, L. Z.; Kroetz, D. L.; Sheiner, L. B. The dynamics of drug absorption distribution and elimination. In *The Pharmacological Basis of Therapeutics*; Goodman, G. A., Gilman, R. H., Eds., 9th ed.; McGraw-Hill: New York, 1996; pp 3–27.
13. Muller, W. E.; Wollert, U. *Pharmacology* **1979**, *19*, 56.
14. Rühl, T.; Daghish, M.; Buchynskyy, A.; Barche, K., et al. *Bioorg. Med. Chem.* **2003**, *11*, 2965.
15. Cui, F. L.; Fan, J.; Li, J. P.; Hu, Z. D. *Bioorg. Med. Chem.* **2004**, *12*, 151.
16. Zhong, W. Y.; Wang, Y. C.; Yu, J. S.; Liang, Y. Q.; Ni, K. Y.; Tu, S. Z. *J. Pharm. Sci.* **2004**, *93*, 1039.
17. Papadopoulou, A.; Green, R. J.; Frazier, R. A. *J. Agric. Food Chem.* **2005**, *53*, 158.
18. Sengupta, B.; Banerjee, A.; Sengupta, P. K. *J. Photochem. Photobiol. B* **2005**, *80*, 79.
19. Mallick, A.; Haldar, B.; Chattopadhyay, N. *J. Phys. Chem. B* **2005**, *109*, 14683.
20. Trynda-Lemiesz, L.; Kozlowski, H. *Bioorg. Med. Chem.* **1996**, *4*, 1709.
21. Dufour, C.; Dangles, O. *Biochim. Biophys. Acta* **2005**, *1721*, 164.
22. Zsila, F.; Bikádi, Z.; Simonyi, M. *Biochem. Pharmacol.* **2003**, *65*, 447.
23. Trynda-Lemiesz, L. *Bioorg. Med. Chem.* **2004**, *12*, 3269.
24. Liu, J. Q.; Tian, J. N.; Tian, X.; Hu, Z. D.; Chen, X. G. *Bioorg. Med. Chem.* **2004**, *12*, 469.
25. Sulkowska, A. *J. Mol. Struct.* **2002**, *614*, 227.
26. Trynda-Lemiesz, L.; Keppler, B. K.; Koztowski, H. J. *Inorg. Biochem.* **1999**, *73*, 123.
27. Lackowicz, J. R. *Principles of Fluorescence Spectroscopy*, 2nd ed.; Kluwer/Plenum: New York, 1999.
28. Goya, S.; Takadate, A.; Fujino, H.; Otagiri, M.; Uekama, K. *Chem. Pharm. Bull.* **1982**, *30*, 1363.
29. Eftink, M. R.; Ghiron, C. A. *J. Phys. Chem.* **1976**, *80*, 486.
30. Miller, J. N. *Proc. Anal. Div. Chem. Soc.* **1979**, *16*, 203.
31. Zhu, J.; Tong, S. Y. *Chem. J. Chin. Univ.* **1996**, *17*, 539.
32. Sirotkin, V. A.; Zinatullin, A. N.; Solomonov, B. N.; Faizullin, D. A.; Fedotov, V. D. *Biochim. Biophys. Acta* **2001**, *1547*, 359.
33. Rahmelow, K.; Hubner, W. *Anal. Biochem.* **1996**, *241*, 5.
34. Jiang, M.; Xie, M. X.; Zheng, D.; Liu, Y.; Li, X. Y.; Chen, X. *J. Mol. Struct.* **2004**, *692*, 71.
35. Sudlow, G.; Birkett, D. J.; Wade, D. N. *Mol. Pharmacol.* **1976**, *12*, 1052.
36. Chen, R. F. *Arch. Biochem. Biophys.* **1974**, *160*, 106.
37. Dockal, M.; Carter, D. C.; Ruker, F. *J. Biol. Chem.* **1999**, *274*, 29303.
38. Suarez Varela, A.; Sandez Macho, M. I.; Minones, J. *J. Pharm. Sci.* **1992**, *81*, 842.
39. Tang, J. H.; Qi, S. D.; Chen, X. G. *J. Mol. Struct.* **2005**, *779*, 87.
40. Bertucci, C.; Domenici, E. *Curr. Med. Chem.* **2002**, *9*, 1463.
41. Scatchard, G. *Ann. N.Y Acad. Sci.* **1949**, *51*, 660.
42. Zhao, B. Z.; Xie, J.; Zhao, J. Q. *Biochim. Biophys. Acta* **2005**, *1722*, 124.
43. Ross, D. P.; Subramanian, S. *Biochemistry* **1981**, *20*, 3096.
44. Sjoholm, I.; Ekman, B.; Kober, A.; Ljungstedt-Pahlman, I.; Seiving, B.; Sjodin, T. *Mol. Pharmacol.* **1979**, *16*, 767.
45. Curry, S.; Mandelkow, H.; Brick, P.; Franks, N. *Nat. Struct. Biol.* **1998**, *5*, 827.
46. Dong, A.; Huang, P.; Caughey, W. S. *Biochemistry* **1990**, *29*, 3303.